

1-1-2014

## Room-temperature spin-polarized organic light-emitting diodes with a single ferromagnetic electrode

Baofu Ding  
*Edith Cowan University*

Qunliang Song

Kamal Alameh  
*Edith Cowan University*

Follow this and additional works at: <https://ro.ecu.edu.au/ecuworkspost2013>



Part of the [Engineering Science and Materials Commons](#)

---

10.1063/1.4879461

This is an Author's Accepted Manuscript of: Ding B., Song Q., Alameh K. (2014). Room-temperature spin-polarized organic light-emitting diodes with a single ferromagnetic electrode. *Applied Physics Letters*, 104(20). Available [here](#)  
This Journal Article is posted at Research Online.  
<https://ro.ecu.edu.au/ecuworkspost2013/333>

## Room-temperature spin-polarized organic light-emitting diodes with a single ferromagnetic electrode

Baofu Ding, Qunliang Song, and Kamal Alameh

Citation: *Applied Physics Letters* **104**, 203302 (2014); doi: 10.1063/1.4879461

View online: <http://dx.doi.org/10.1063/1.4879461>

View Table of Contents: <http://scitation.aip.org/content/aip/journal/apl/104/20?ver=pdfcov>

Published by the AIP Publishing

---

### Articles you may be interested in

[Manganese-doped indium oxide and its application in organic light-emitting diodes](#)

*Appl. Phys. Lett.* **99**, 023302 (2011); 10.1063/1.3610559

[Organic light-emitting diode with liquid emitting layer](#)

*Appl. Phys. Lett.* **95**, 053304 (2009); 10.1063/1.3200947

[Efficient, single-layer molecular organic light-emitting diodes](#)

*Appl. Phys. Lett.* **90**, 023511 (2007); 10.1063/1.2426882

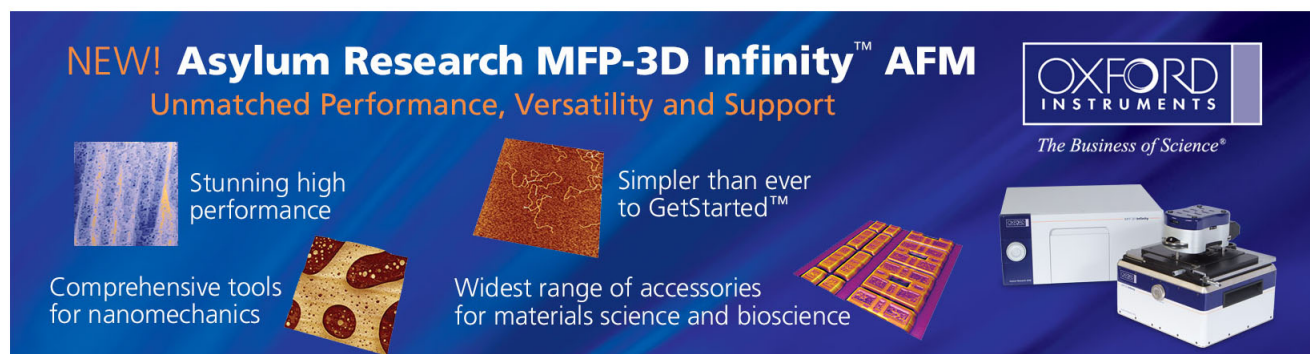
[Doped thin films of two organic molecules for light-emitting diodes](#)

*Appl. Phys. Lett.* **83**, 4318 (2003); 10.1063/1.1630156

[Organic light emitting diodes with spin polarized electrodes](#)

*J. Appl. Phys.* **93**, 7682 (2003); 10.1063/1.1556118

---

This is a promotional banner for the Asylum Research MFP-3D Infinity AFM. The background is dark blue. On the left, there are three small images: a blue textured surface, a brown textured surface, and a yellow and red patterned surface. To the right of these images are three text blocks: 'Stunning high performance', 'Simpler than ever to GetStarted™', and 'Widest range of accessories for materials science and bioscience'. Below the first two text blocks is a fourth text block: 'Comprehensive tools for nanomechanics'. On the far right, there is a large image of the MFP-3D Infinity AFM instrument, which is a white and blue boxy device with a smaller unit on top. Above the instrument is the Oxford Instruments logo, which consists of the word 'OXFORD' in a large, white, serif font above the word 'INSTRUMENTS' in a smaller, white, sans-serif font. Below the logo is the tagline 'The Business of Science®'.

# Room-temperature spin-polarized organic light-emitting diodes with a single ferromagnetic electrode

Baofu Ding,<sup>1,a)</sup> Qunliang Song,<sup>2</sup> and Kamal Alameh<sup>1,b)</sup>

<sup>1</sup>*Electron Science Research Institute, Edith Cowan University, 270 Joondalup Drive, Joondalup WA 6027 Australia*

<sup>2</sup>*Institute for Clean Energy and Advanced Materials, Southwest University, Chongqing 400715, People's Republic of China*

(Received 17 February 2014; accepted 11 May 2014; published online 21 May 2014)

In this paper, we demonstrate the concept of a room-temperature spin-polarized organic light-emitting diode (Spin-OLED) structure based on (i) the deposition of an ultra-thin p-type organic buffer layer on the surface of the ferromagnetic electrode of the Spin-OLED and (ii) the use of oxygen plasma treatment to modify the surface of that electrode. Experimental results demonstrate that the brightness of the developed Spin-OLED can be increased by 110% and that a magneto-electroluminescence of 12% can be attained for a 150 mT in-plane magnetic field, at room temperature. This is attributed to enhanced hole and room-temperature spin-polarized injection from the ferromagnetic electrode, respectively. © 2014 AIP Publishing LLC. [<http://dx.doi.org/10.1063/1.4879461>]

Since 1987, organic light-emitting diodes (OLEDs) have been intensively investigated and greatly improved in performance.<sup>1</sup> In a conventional OLED, electrons and holes have random spin directions. According to the spin statistic theory of carrier recombination, for conventional OLEDs, the ratio between the generated singlet excitons and triplet excitons is 1:3, due to the random orientation of spin injection, as shown in Fig. 1(a). Owing to the weak spin-orbit coupling in most organic semiconductors, only singlet excitons contribute to light emission, then the maximum internal quantum efficiency of conventional OLEDs cannot exceed 25%. Spin-polarized OLEDs (Spin-OLEDs) are receiving great attention because of their ability to achieve high brightness with low power consumption. By injecting spin-polarized carriers from ferromagnetic electrodes, the exciton spin statistics, and hence light emission, can be controlled.<sup>2</sup> In principle, if two electrodes are spin-polarized and aligned in parallel, the spin states for electrons and holes generate singlet and triplet states with a 0:4 ratio, as illustrated in Fig. 1(b). In this case, the lack of singlet excitons in the organic emissive layer results in zero charge-to-photon conversion efficiency. However, if the two electrodes of the OLED are spin-polarized and aligned in antiparallel, the spin states for electrons and holes generate singlet and triplet states with a ratio of 2:2 as shown in Fig. 1(c). In this case, the maximum internal quantum efficiency increases to 50%. Therefore, it is feasible to realise the magnetically modulated electroluminescence from a Spin-OLED.

To achieve the goal, Vardeny's group recently developed a Spin-OLED based on the use of ferromagnetic  $\text{La}_{0.7}\text{Sr}_{0.3}\text{MnO}_3$  (LSMO) electrode, demonstrating a spin-polarized-injection-induced magneto-electroluminescence (MEL) of 1% at 10 K ( $-263^\circ\text{C}$ ).<sup>3</sup> This observation validated the ability of spin-polarized injectors to modulate the EL of OLEDs. However, all Spin-OLED demonstrators reported to

date have major limitations, namely, weak emission, weak MEL, and low-temperature operation, which are prohibiting product-level development.

It is important to note that the magnetic LSMO has mainly been proposed as an ideal transparent spin-polarised hole injector due to its (i) high work function, (ii) relative high transparency, and (iii) high Curie Temperature ( $>300\text{ K}$ ).<sup>3,4</sup> However, the existence of oxygen vacancy on the LSMO electrode surface as well as the dipole interaction between this magnetic electrode and the organic layer have not only limited the EL of the OLED but also reduced the correlation between the magnetic field and the EL at room temperature.<sup>5</sup>

In this paper, we adopt an approach based on the use of oxygen plasma for treating the LSMO electrode surface, in conjunction with the deposition of an ultra-thin p-type buffer layer for modifying the surface of LSMO magnetic electrode. Experimental results demonstrate a substantial increase of 110% in brightness and a magneto-electroluminescence of 12%, for an external magnetic field of 150 mT at room-temperature. The experimental results represent a solid step towards the development of magnetically controlled flat panel displays.

LSMO magnetic electrodes were grown, using channel-spark ablation and polycrystalline targets, on three different (100)-oriented transparent  $\text{SrTiO}_3$  (STO) substrates. The growth method is described in detail in Ref. 6. A shadow mask with a width of approximately 2 mm was used during the growth process to produce strip-shaped LSMO films.

Prior to treatment, the STO/LSMO substrates were ultrasonically cleaned in ethanol (3 min) and acetone (2 min) in turn. The surface modification steps were as follows:

- (1) Having been chemically cleaned by acetone, the LSMO samples were introduced into the preparation chamber for further treatments in vacuum, including annealing in ultra-high vacuum and exposure to the activated oxygen. To maintain a uniform surface stoichiometry, the annealing temperature was never increased beyond

<sup>a)</sup>Electronic mail: b.ding@ecu.edu.au

<sup>b)</sup>Electronic mail: k.alameh@ecu.edu.au

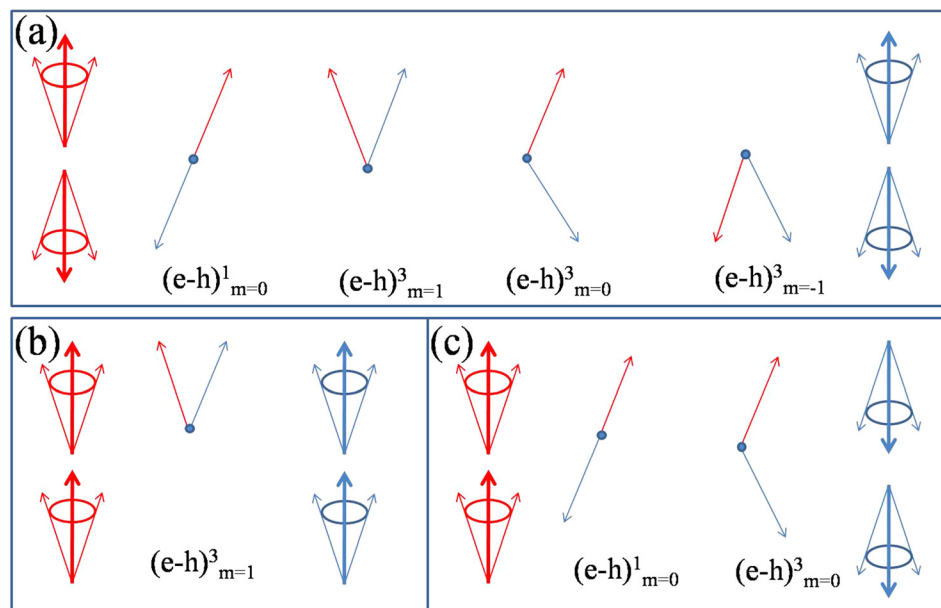


FIG. 1. Spin statistics of excitons formed in (a) a conventional OLED without spin polarized injection, (b) a spin-OLED with spin-polarized injection in the parallel alignment, and (c) a spin-OLED with spin-polarized injection in the antiparallel alignment.

450 °C. During the oxygen plasma treatment, the pressure was kept at  $4 \times 10^{-3}$  Pa. To activate oxygen, a thin stainless steel rod pointing to the metallic sample holder edge was mounted inside each of the preparation chambers. The rod could be driven close to the sample holder edge so that a dc discharge could be generated at very low applied voltages when oxygen was let in at an appropriate pressure. Care was taken to avoid any damage of the LSMO surface by the accelerated ions.

- (2) Immediately after oxygen plasma treatment, the samples were transferred into the growth chamber with a base pressure of  $5 \times 10^{-5}$  Pa for subsequent deposition of a p-type buffer layer Tetrafluoro-tetracyanoquinodimethane (F4-TCNQ), which was especially chosen to increase the hole injection efficiency.

After the two-step treatment, tris-(8-hydroxyquinoline) aluminum ( $\text{Alq}_3$ ) and N,N'-bis(1-naphthyl)-N,N'-diphenyl-1,1'-biphenyl-4,4'-diamine (NPB) were, respectively, chosen as the electron-transporting and light-emitting layer and the hole-transporting layer, and aluminum was chosen as the cathode. To increase the electron injection efficiency, a thin layer of LiF buffer was inserted between the Al and  $\text{Alq}_3$  layers, as typically done in conventional OLEDs. The top Al layer was a 1 mm wide narrow strip, crossing the bottom 2-mm LSMO strip, thus forming an active device area of approximately  $1 \times 2 \text{ mm}^2$ . The device with oxygen plasma treatment and F4-TCNQ deposition is named as OF-Spin-OLED, and its structure is represented as  $\text{STOLSMO (20 nm)} \backslash \text{F4-TCNQ (1 nm)} \backslash \text{NPB (15 nm)} \backslash \text{Alq}_3 (80 \text{ nm}) \backslash \text{LiF (0.8 nm)} \backslash \text{Al (100 nm)}$ . For comparison purposes, two more devices were fabricated, namely, a control spin-OLED (C-Spin-OLED) without any surface treatment and a Spin-OLED with only oxygen plasma treatment (O-Spin-OLED). The structures of the C-Spin-OLED, O-Spin-OLED, and OF-Spin OLED are schematically shown in Fig. 2(a). Measured device characteristics were taken in a nitrogen glove box with both  $\text{H}_2\text{O}$  and  $\text{O}_2$  contents less than 1 ppm. Magnetic fields were applied by switching on/off an electromagnet, either parallel or perpendicular to the device

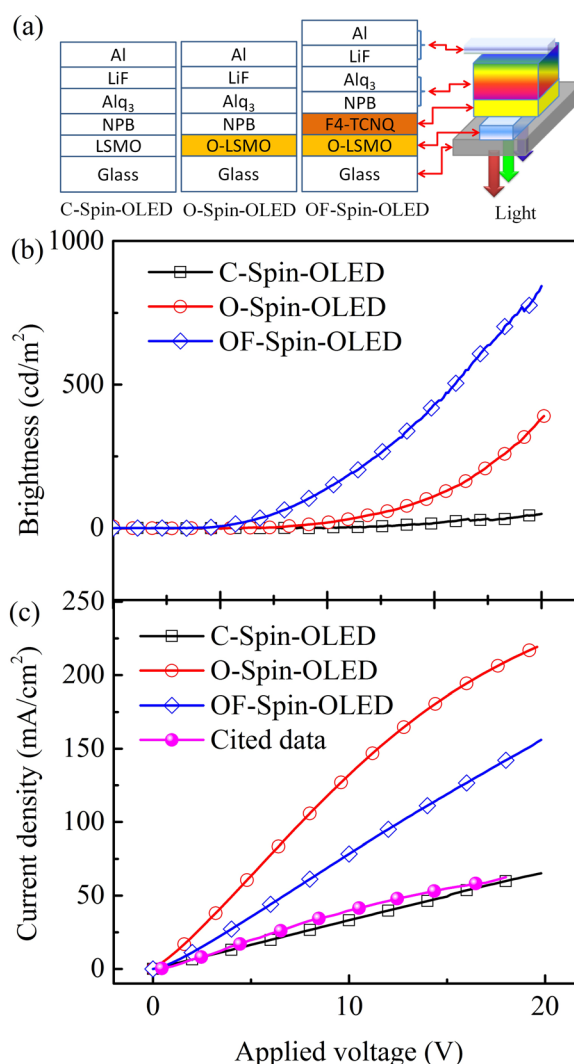


FIG. 2. (a) Developed C-Spin-OLED, O-Spin-OLED, and OF-Spin-OLED structures, and their (b) brightness vs voltage and (c) current vs voltage characteristics.



surface. The photodiode used for EL measurement was magnetically shielded.

Figs. 2(b) and 2(c) show the Brightness-Current density-Voltage (B-I-V) characteristics of the three devices shown in Fig. 2(a). It is obvious from Fig. 2(b) that the C-Spin-OLED exhibits the same I-V characteristics as those reported by Dediu.<sup>6</sup> This agreement in I-V characteristics confirmed the accuracy of our developed C-Spin-OLED structure. Fig. 2(b) shows that for the O-spin-OLED, the current density is much higher than that of the C-Spin-OLED, which in turn, leads to much higher brightness of 350 cd/m<sup>2</sup> at an operating voltage of about 20 V. For OF-Spin-OLED, the current density at a given forward-bias voltage is between that of the C-Spin-OLED and that of the O-Spin-OLED. However, the brightness of the OF-Spin-OLED is higher than that of the O-Spin-OLED, reaching around 800 cd/m<sup>2</sup> at 20 V. This is by far the highest measured brightness attained by an LSMO-based Spin-OLED. All previously reported B-V data have been in “arb. units” or, representing quite low absolute intensities actually. Since the cathode of the proposed OF-Spin-OLED is the same as that reported in Refs. 4 and 6, it is reasonable to attribute the enhancement in light emission to the improved electronic properties at the Anode/Organic Semiconductor interface, attained through the surface treatment of the LSMO surface.

To simulate the effect of the oxygen plasma treatment and the P-type F4-TCNQ buffer layer deposition on the B-I-V characteristics of the developed Spin-OLEDs, we adopted the circuit model, shown in Fig. 3(a), which was reported in Ref. 7. The circuit model consists of three components, namely, a series resistance  $R_s$ , an inter-electrode leak resistance  $R_L$ , and voltage-dependent diode of impedance  $Z_D$ . The sheet resistance of the LSMO film is the dominant contributor to  $R_s$ . Fig. 3(b) shows a real photograph of the light emitted from the developed OF-Spin-OLED during operation. It is obvious that the device has two separated areas, namely: a Dark-Spot Area (DSA) and a Light-Emitting Area (LEA). The DSA is attributed to the uneven surface roughness of the LSMO electrode which results in thick LSMO islands over which the thickness of the active organic layer is negligible, leading to localized leakage currents and dark spots.<sup>4,6,7</sup> The inter-electrode leak resistance of this DSA is referred as  $R_L$ . On the other hand, the LEA is governed by the voltage-dependent impedance of the diode, thus emitting light with a brightness profile that depends on the effective

thickness profile of the active organic layer. According to this circuit model and Fig. 2(b), for a forward-bias voltage exceeding the threshold voltage of  $Z_D$ , the I-V curve exhibits an ohmic-like behavior of slope  $R_s$ .

Zhan *et al.* have recently found that when an untreated LSMO electrode is in contact with an organic semiconductor material, a strong interface dipole is formed, which shifts down the whole energy diagram of the organic semiconductor with respect to the vacuum level.<sup>8</sup> This increases the hole injection barrier, thus increasing the threshold voltage of voltage-dependent diode. In this case, the C-Spin-OLED has near-zero light emission even for an applied forward-bias voltage of 20 V. Another recent study has revealed that exposure of the LSMO surface to activated oxygen can raise its work function (WF) from 4.6 eV to 5.1 eV, thus lowering the hole injection barriers.<sup>9</sup> In this case, switching the LEA requires a turn-on voltage as low as 11 V, as shown in Fig. 2(b). Below 11 V, negligible light emission from the O-Spin-OLED is observed since most of the current flows through DSA. Once the applied voltage exceeds 11 V,  $Z_D$  significantly decreases, thus enabling a higher current to flow through the LEA. For the OF-Spin-OLED, one can see from Fig. 2(b) that the turn-on voltage can be further reduced from 11 V to 5 V, and that the brightness at 20 V is as high as 800 cd/m<sup>2</sup>. Due to its high Lowest Unoccupied Molecular Orbital (LUMO)-to-Vacuum Level energy gap, F4-TCNQ has been proposed as a potential p-type dopant for OLEDs and demonstrated for a variety of optoelectronic applications.<sup>10</sup> Especially, F4-TCNQ has been used to increase the work function of electrodes, such as Graphene, Carbon Nanotube, Al, and Au. The increase in work function is mainly due to charge transfer from the electrode to the F4-TCNQ molecules. Also, since the LUMO of F4-TCNQ is typically lower than the Highest Occupied Molecular Orbital (HOMO) of the hole transporting organic materials (denoted NPB in Fig. 2(a)), the electron transfer from NPB to F4-TCNQ becomes more favorable. The holes generated in the process participate in the charge transport thus resulting in an increase in device conductivity. No matter which mechanism is dominant (increasing work function or hole conductivity), the hole injection is always improved with the insertion of a 1-nm thick F4-TCNQ layer, thus increasing the LEA and reducing the DSA.

It is important to note that the MEL performance of conventional OLEDs employing non-magnetic electrodes have been reported for almost a decade.<sup>11–13</sup> However, the origin of the MEL is still not fully understood. No matter whether the MEL is determined by the magnetic field influenced exciton formation or by the bipolaron formation, both mechanisms take place in the bulk of the organic layers of conventional OLEDs. Therefore, it is logical to consider the MEL of conventional OLEDs as an organic bulk effect. To calculate the MEL related to the organic bulk effect, we fabricated an OLED structure similar to that of the C-Spin-OLED, but with the LSMO ferromagnetic electrode replaced with a non-magnetic ITO electrode. Figs. 4(b) and 4(c) show the brightness of the conventional OLED and OF-Spin-OLED for on/off switching by out-of-plane or in-plane magnetic fields of intensity 150 mT (Fig. 4(a)), for an applied voltage of 12 V. In Fig. 4(b), negligible change in brightness

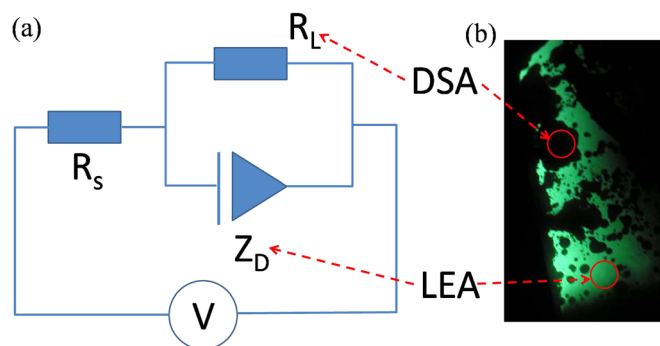


FIG. 3. (a) Equivalent circuit and (b) photograph showing the light emitted from the OF-Spin-OLED device driven by a forward-bias voltage of 13 V.

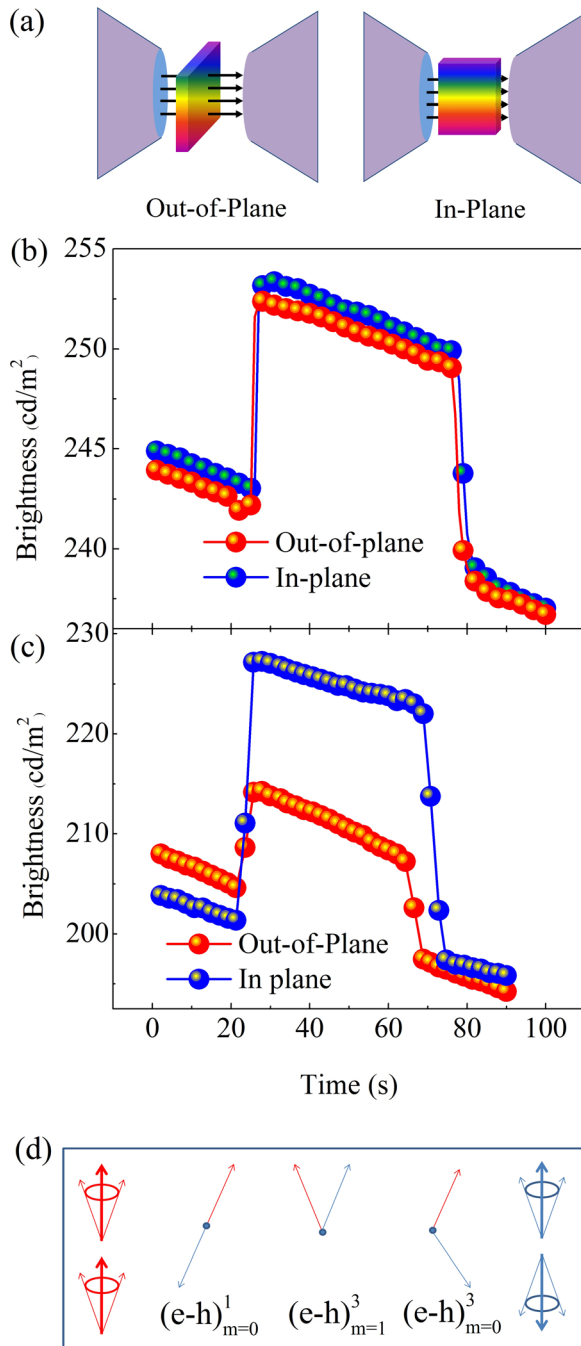


FIG. 4. (a) Illustration of out-of-plane and in-plane magnetic fields applied onto an OLED. Brightness versus time for (b) OLED with nonmagnetic electrodes and (c) OF-Spin-OLED, during on/off switching with a magnetic field of 150 mT, for an applied voltage of 12 V. (d) Spin statistics of excitons formed in a Spin-OLED with one ferromagnetic electrode.

is observed when the magnetic field direction is switched from in-plane to out-of-plane, making the MEL independent of the magnetic field direction. On the other hand, for the OF-Spin-OLED, the brightness is sensitive to the orientation of the magnetic field as shown in Fig. 4(c). Defining the MEL as  $(EL(B) - EL(0)) / EL(0)$ , where  $EL(B)$  is the brightness at a magnetic field  $B$ , it is obvious from Fig. 4(c) that 5.2% MEL and 12.2% MEL are achieved for out-of-plane and in-plane magnetic fields, respectively, whereas the MEL of the conventional OLED is around 4.4% (as calculated from Fig. 4(b)). One may notice that the null field baselines of the brightness curves display slight decays over the

measurement time. These are partly due to the heat generated in both the DSA and LEA, which reduces the brightness of the LEA.

Note that a recent study on the magnetic hysteresis loop of a 20 nm-thick LSMO film deposited onto STO demonstrates that the in-plane and out-of-plane applied magnetic fields are along the easy axis and hard axis of the magnetization, respectively, at room temperature.<sup>14,15</sup> Therefore, for the 20-nm-thick LSMO film used in the experiment, an in-plane 150 mT magnetic field was sufficient to saturate its in-plane magnetization; while, for the out-of-plane orientation, a much higher field was needed to saturate the magnetization, which can also be proved by the different magnetoresistances of LSMO in the in-plane and out-of-plane magnetic fields with the same intensity. Therefore, in-plane orientation results in higher spin polarization and lower electrode resistance. Separate measurements of the current flowing along a bare LSMO electrode surface also show that the current is increased by 2.6% and 1.1% (not plotted) for the in-plane and out-of-plane magnetic fields, respectively. Therefore, the in-plane magnetic field provides additional 1.5% increase in Spin-OLED current with respect to the increment in current generated by the out-of-plane magnetic field. This additional 1.5% in current results in 4.0% in MEL (see supplementary material<sup>16</sup>). Adding this 4.0% increase in MEL to the 5.2% MEL of a Spin-OLED driven by an out-of-plane magnetic field leads to an overall MEL of 9.2%. Since the measured MEL for an in-plane magnetic field is 12.2% (Fig. 4(c)), the spin-polarized hole injection contributes the extra 3.0% MEL for in-plane magnetic field. Note that this result is different from that reported in Ref. 7, where the increase in MEL for the in-plane magnetic field is merely attributed to the decrease in  $R_s$ .

Unlike the Spin-OLED with two magnetic electrodes, the OF-Spin-OLED reported in this paper has only one magnetic electrode. Fig. 4(d) illustrates the exciton formation in the case of the spin polarized injection from only one magnetic electrode. When spin-polarized holes from the LSMO electrode and non-spin-polarized electrons from the Al electrode recombine, they give rise to only three exciton states, namely,  $(e-h)^1_{m=0}$ ,  $(e-h)^3_{m=0}$ , and  $(e-h)^3_{m=1}$ , with a ratio profile of 1:1:2 as shown in Fig. 3(b). This is based on the assumption that the spin-up and spin-down electrons are paired with the spin-up holes with identical probabilities through wave function combinations. Considering that (i) population of excitons in three states of  $(e-h)^1_{m=0}$ ,  $(e-h)^3_{m=0}$ , and  $(e-h)^3_{m=1}$  are extremely unbalanced and (ii) mutual singlet-triplet intersystem conversion can occur through singlet-triplet crossing or triplet-triplet annihilation,<sup>17,18</sup> the unbalanced triplet and singlet excitons can be redistributed through the mutual intersystem conversion. At equilibrium, the ratio profile of  $(e-h)^1_{m=0}:(e-h)^3_{m=0}:(e-h)^3_{m=1}$  is 1:1:1.

Compared to non-spin-polarized hole injection, spin polarized injection increases the singlet exciton fraction from 1/4 to 1/3 leading to a higher EL efficiency in external magnetic fields. Note that all our measurements were carried out at room temperature. It is important to note that when the temperature of the LSMO electrode,  $T$ , is less than  $T_C$  (Currie temperature), the Mn 3d electron spins are aligned ferromagnetically owing to the ferromagnetic

double-exchange interaction. Thus, the Mn 3d states, which extend above the Fermi level, contribute only majority spins. However, the O 2p states, which have both majority and minority spins, are only 0.6 eV below the Fermi level. Therefore, the majority-spin states behave like those of metal injecting charge carriers from the Mn 3d states, whereas the minority-spin states behave like those of an insulating gap between the occupied O 2p states and the unoccupied Mn 3d minority-spin states. Thus, the density of states near the Fermi level is spin-polarized.<sup>19</sup> Noticeably, a recent study has revealed that the Curie temperature of LSMO thin films can be increased from 278 K (below room temperature) to 310 K, which is above room-temperature, by annealing the LSMO film in oxygen gas to increase the stoichiometric oxygen content. The increased Curie temperature is due to the hole doping effect of oxygen excess in a sub-optimum ( $x < 0.33$ ) cationic strontium doped phase. Therefore, oxygen plasma treatment increases the stoichiometric oxygen content in LSMO film, leading to a pronounced increase in Curie temperature. Characterizing the effect of oxygen treatment on the magnetic properties of LSMO is beyond the scope of this paper and will therefore be investigated and reported elsewhere.<sup>20</sup> Finally, it is important to state that the reported Curie temperature for oxygen-gas treated LSMO is higher than the room temperature, making spin-polarized hole injection from LSMO dominant at room-temperature, and leading to the extra 3.0% increase in MEL, discussed earlier.

We have proposed and demonstrated the concept of a room-temperature Spin-OLED structure based on a material processing approach combining the deposition of an ultra-thin p-type organic buffer layer on the surface of the ferromagnetic electrode of the spin-OLED and the use of oxygen plasma treatment for electrode surface modification. Experimental results have shown that the use of treated LSMO ferromagnetic electrode enhances hole injection and room-temperature spin-polarized injection. Also, experimental results have demonstrated an enhancement in brightness by 110% and a magneto-electroluminescence of 12.2% for a 150 mT in-plane magnetic field. The proposed Spin-OLED

has application in magnetic-field-controlled flat panel displays.

This work research was supported by Edith Cowan University, the Department of Industry, Innovation, Science, Research and Tertiary Education, Australia. This work was also supported by the National Natural Science Foundation of China (Grant No. 11274256).

- <sup>1</sup>C. W. Tang and S. A. Vanslyke, *Appl. Phys. Lett.* **51**, 913 (1987).
- <sup>2</sup>V. Dediu, M. Murgia, F. C. Matocotta, C. Taliani, and S. Barbanera, *Solid State Commun.* **122**, 181 (2002).
- <sup>3</sup>T. D. Nguyen, E. Ehrenfreund, and Z. V. Vardeny, *Science* **337**, 204 (2012).
- <sup>4</sup>I. Bergenti, V. Dediu, M. Murgia, A. Riminucci, G. Ruani, and C. Taliani, *J. Lumin.* **110**, 384 (2004).
- <sup>5</sup>S. Picozzi, C. Ma, Z. Yang, R. Bertacco, M. Cantoni, A. Cattoni, D. Petti, S. Brivio, and F. Ciccacci, *Phys. Rev. B* **75**, 094418 (2007).
- <sup>6</sup>E. Arisi, I. Bergenti, V. Dediu, M. A. Loi, M. Muccini, M. Murgia, G. Ruani, C. Taliani, and R. Zamboni, *J. Appl. Phys.* **93**, 7682 (2003).
- <sup>7</sup>B. F. Ding, Y. Q. Zhan, Z. Y. Sun, X. M. Ding, X. Y. Hou, Y. Z. Wu, I. Bergenti, and V. Dediu, *Appl. Phys. Lett.* **93**, 183307 (2008).
- <sup>8</sup>Y. Q. Zhan, I. Bergenti, L. E. Hueso, V. Dediu, M. P. de Jong, and Z. S. Li, *Phys. Rev. B* **76**, 045406 (2007).
- <sup>9</sup>X. Z. Wang, X. M. Ding, Z. S. Li, Y. Q. Zhan, I. Bergenti, V. A. Dediu, C. Taliani, Z. T. Xie, B. F. Ding, X. Y. Hou, W. H. Zhang, and F. Q. Xu, *Appl. Surf. Sci.* **253**, 9081 (2007).
- <sup>10</sup>W. Chen, S. Chen, D. C. Qi, X. Y. Gao, and A. T. S. Wee, *J. Am. Chem. Soc.* **129**, 10418 (2007).
- <sup>11</sup>P. A. Bobbert, T. D. Nguyen, F. W. A. van Oost, B. Koopmans, and M. Wohlgenannt, *Phys. Rev. Lett.* **99**, 216801 (2007).
- <sup>12</sup>B. F. Ding, Y. Yao, Z. Y. Sun, C. Q. Wu, X. D. Gao, Z. J. Wang, X. M. Ding, W. C. H. Choy, and X. Y. Hou, *Appl. Phys. Lett.* **97**, 163302 (2010).
- <sup>13</sup>B. Hu and Y. Wu, *Nature Mater.* **6**, 985 (2007).
- <sup>14</sup>P. Perna, C. Rodrigo, E. Jiménez, F. J. Teran, N. Mikuszeit, L. Méchin, J. Camarero, and R. Miranda, *J. Appl. Phys.* **110**, 013919 (2011).
- <sup>15</sup>E. P. Houwman, G. Maris, G. M. De Luca, N. Niermann, G. Rijnders, D. H. A. Blank, and S. Speller, *Phys. Rev. B* **77**, 184412 (2008).
- <sup>16</sup>See supplementary material at <http://dx.doi.org/10.1063/1.4879461> for additional experimental details on the relationship between current change and brightness change.
- <sup>17</sup>Y. Wu, B. Hu, J. Howe, A.-P. Li, and J. Shen, *Phys. Rev. B* **75**, 075413 (2007).
- <sup>18</sup>B. F. Ding, Y. Yao, C. Q. Wu, X. Y. Hou, and W. C. H. Choy, *J. Phys. Chem. C* **115**, 20295 (2011).
- <sup>19</sup>J. H. Park, E. Vescovo, H. J. Kim, C. Kwon, R. Ramesh, and T. Venkatesan, *Nature* **392**, 794 (1998).
- <sup>20</sup>T. Petrisor, M. S. Gabor, A. Boule, C. Bellouard, C. Tiusan, O. Pana, and T. Petrisor, *J. Appl. Phys.* **109**, 123913 (2011).